

# Ultrasonically Driven Surface Micromachined Motor

Ville Kaajakari<sup>a)</sup>, Steve Rodgers<sup>b)</sup>, and Amit Lal<sup>a)</sup>

*a)*Department of Electrical and Computer Engineering, University of Wisconsin Madison,  
1415 Engineering Dr., Madison, Wisconsin, 53706  
[lal@engr.wisc.edu](mailto:lal@engr.wisc.edu)

*b)* Intelligent Micromachine Department,  
Sandia National Lab., Albuquerque, New Mexico, 86185

## ABSTRACT

The first-ever all-surface micromachined ultrasonic micro-rotor is presented. The rotor is actuated by electrically driving a piezoelectric PZT (lead-zirconate-titanate) plate mounted at the back of the silicon die eliminating the need for interconnects and space consuming surface actuators. The rotor operates with a single phase sub-five volt peak-to-peak excitation in atmospheric pressure. The piezoelectric plate is adhesively mounted making the method suitable for actuating micromachines from any surface micromachining process. Two different modes of operation are demonstrated: pulsed and resonant. The pulse actuation results in low rotation rate (0.5-3 RPM) while resonant actuation results in a fast rotation (10-100 RPM). The ability to drive a geared down rotor (50:7), much smaller than the driving rotor, indicates high torque output capability.

## I. INTRODUCTION

This paper reports on the first ever *surface micromachined* ultrasonic rotor. Historically, macro scale ultrasonic motors have been used in applications like portable autofocus cameras requiring small form [1]. Compared to the conventional electromagnetic motors, ultrasonic motors have a large torque-to-speed ratio eliminating the need for gear reduction. They also have a large hold-on torque without requiring energy consumption. Ultrasonic actuation is based on frictional coupling of vibrations from a piezoelectric actuator to a rotor. Since the rotor does not have to be conductive, a wider choice of rotor material is possible, as compared to the electrostatic, magnetic, or thermally driven micromotors.

Moroney *et al.* reported on ultrasonic actuation of polysilicon particles using flexural plate waves (FPWs) on silicon nitride membranes [2, 3]. Flynn *et al.* also recognized the advantages of piezoelectric materials for microrotor actuation [4, 5]. The devices by Flynn *et al.* consisted of a bulk micromachined nitride membrane actuated by a sol-gel PZT (lead-zirconate-titanate) thin film. The rotor was not integrated in the fabrication process but was manually placed on the nitride membrane. One limitation of these

approaches is that they require bulk micromachining to define the low-stress silicon nitride membranes. In addition, these devices require thin piezoelectric films, which are hard to put down. Special processing of piezoelectric film can be costly and conflict with cleanliness requirements of an IC fabrication facility.

Our approach has been to use commercially available ceramic PZT plates for micromachine actuation. Bulk PZT plates have previously been used to actuate bulk micromachined devices such as silicon based ultrasonic surgical tools [6] and liquid pumps [7]. We have previously reported on using ultrasonic pulses, generated in such composites, for release, assembly, and actuation of surface micromechanical flaps and beams [8, 9]. Specifically, we released stuck polysilicon beams and raised micromachined hinged flaps to an upright position using stress pulses generated by a piezoelectric plate as illustrated in figure 1.

The PZT plate is of similar shape and size as the die and the composite can be mounted in a standard IC package. Bulk silicon processing is not required. Since the plate is mounted at the back of the die *after* surface micro-machine processing, the method is suitable for actuating devices from *any* surface micromachining process. Furthermore, interconnectless actuation of sealed micromachines is possible.

The rotor was fabricated using the Sandia SUMMiT-IV polysilicon surface micromachining process and actuated with a PZT plate (see figure 2). Two different means of excitation are studied: pulsed and resonant. The pulsed ac-

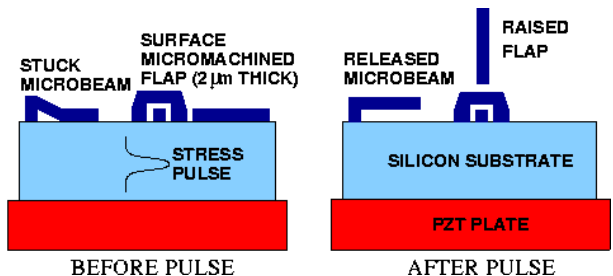


Figure 1: Surface micromachine actuation using stress pulses [8, 9]

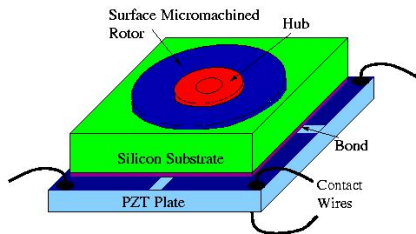


Figure 2: Surface micromachined rotor actuated with PZT plate

tuation is suitable for low speed actuation with RPM ranging from 0.5 to 3 RPM. Resonant actuation results in fast rotation with typical RPM ranging from 10 to 100 RPM. The theory of operation, fabrication process, and experimental results are discussed. The effect of drive voltage, frequency, and operating pressure are identified.

## II. MECHANISMS OF ULTRASONIC ACTUATION

The operation of the ultrasonic microrotor is categorized in four regimes of operation. They are pulsed actuation under vacuum and STP (standard temperature and pressure), and resonant operation in vacuum and STP. Depending on the regime of operation, three different phenomenon are possible: stick-slip due to friction, acoustic streaming, and impact coupling. For frictional coupling the rotation velocity is linearly dependent on vibration amplitude, while for streaming the relationship will be quadratically non-linear [2].

### A. Pulsed drive

In pulsed operation the electric field across the piezoelectric plates result in stress pulses generated at the PZT/adhesive/silicon interfaces. These pulses travel through the composite acoustic waveguide and approaches the silicon surface. Since the analytical formulation of the problem is quite challenging, a finite-element finite-time domain program (PZFlex from Weidlinger Associates) was used to simulate the pulses. Figure 3 shows the silicon surface amplitude as a function of pulse duration. The increase in the surface displacement resulting from increase in pulse duration from 100 ns to 600 ns indicates that the addition of the multiply reflected pulses results in a optimum pulse timing for pulsed actuation of approximately 600 ns. Moreover, as shown in the multiple cycles after pulsing in figure 3, pulse widths between 300 and 600 ns excite the resonances of the PZT/adhesive/silicon composite.

The pulse actuation consist of two steps. In the first step, the silicon surface impacts the free rotor causing it to lift from the die surface towards the hub. In the second step, the free rotor interacts with the compliant hub either by direct impact transfer (in vacuum) or through combination of impact transfer and acoustic streaming (in STP). Since

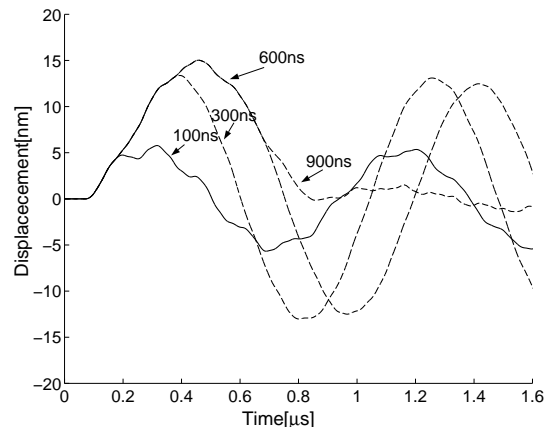


Figure 3: Simulated silicon surface displacement for different pulse widths

the neither the rotor placement nor the pulse amplitude are exactly symmetric with respect to the motor axis, there is a preferred direction for the rotor to move as a result of the impact forces. In particular, the rotor-hub lateral gap of 1 micron allows for it to receive asymmetric forces causing it to rotate. Indeed the problem of pulse interaction with the rotor is a complicated one requiring additional measuring techniques.

### B. Resonant Drive

When the PZT/Si composite plate is driven at resonance, the surface displacement is amplified by the quality factor of the resonator. Much higher displacements are possible at lower drive voltages. The actuation is based on exciting traveling waves on rotor and the hub as shown in figure 4. The resonant modes are excited by driving the PZT/Si composite at the natural frequency or multiple of the hub resonance frequency. The hub resonances become rotating standing waves due to the interaction with rotor and the pulses from the silicon substrate. In this mode mode of operation, the hub becomes the micromotor stator. The hub resonant modes are clearly observed in our experiments when the composite is driven in vacuum. At STP the resonant modes are damped resulting in reduced rotation rate.

## III. DEVICE FABRICATION

Figure 5 shows a schematic and picture of the rotor. The diameter of the  $2.5 \mu\text{m}$  thick rotor is  $1000 \mu\text{m}$ . The rotor was designed to drive smaller gear thus demonstrating an operating microengine with 50:7 gear ratio. In experiments, however, the small gear sometimes broke away during high speed rotation. The gear was therefore removed for rotation speed measurements to remove the uncertainty of gear detachment. The rotor was fabricated using Sandia's SUMMiT four level polysilicon surface micromachining process [10] and released using critical

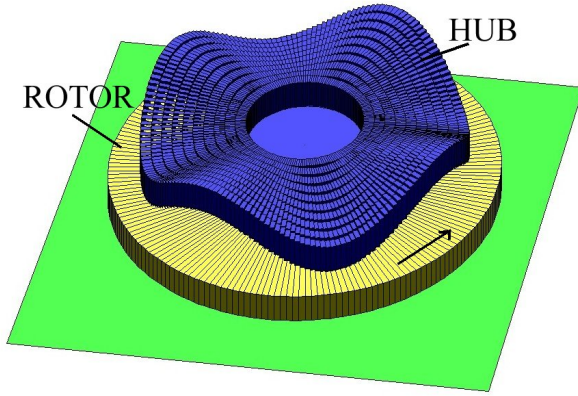


Figure 4: Hub resonance actuating the rotor

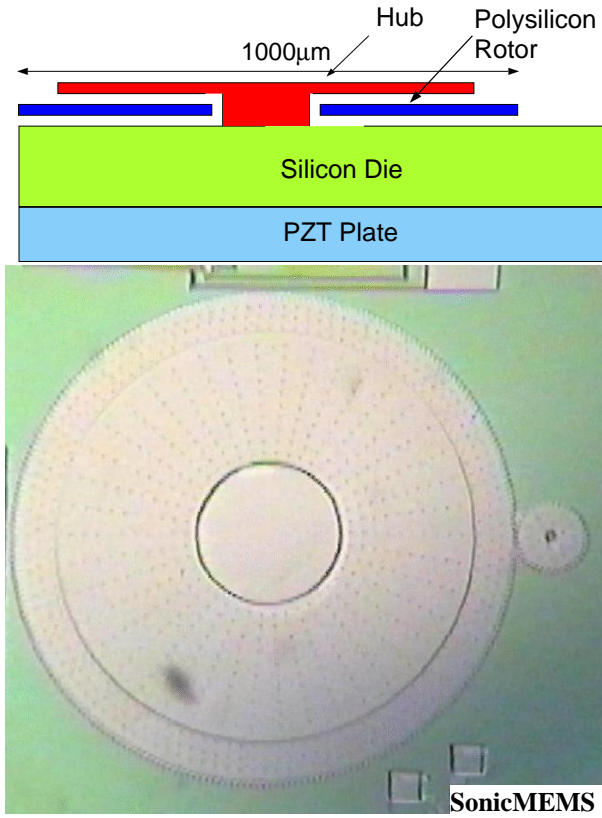


Figure 5: Polysilicon rotor fabricated using SUMMiT process

point drying. No lubricating coating was used to prevent stiction. After release a a rectangular PZT5 plate (10 mm·10 mm·0.3 mm) was mounted on the back of the die using cyanoacrylate. The PZT5 has a high piezoelectric coefficient but is lossy compared to PZT4. It is therefore good choice for pulsed actuation but not as good for resonant actuation where losses dominate the power dissipation. Finally wires were soldered on the corner of the PZT plate.

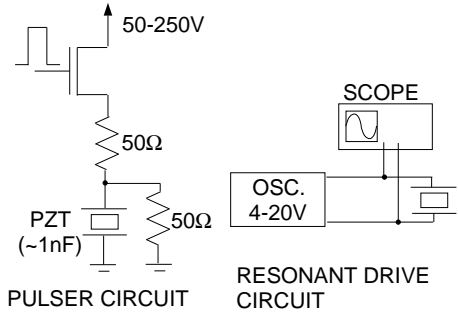


Figure 6: Driving circuits used for actuation

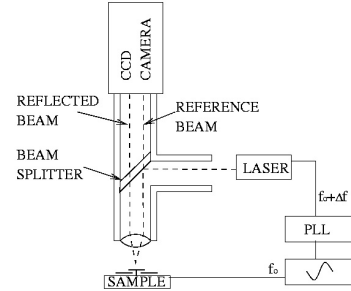


Figure 7: Interferometer and high speed camera set-up

#### IV. EXPERIMENTAL SETUP

To characterize the rotor, it was mounted in a vacuum chamber and the rotation speed was measured using a high speed camera with a 1000 fps maximum sampling rate. The vacuum pressure could be controlled with the pressure range of 60 mTorr to 760 Torr. The driving circuits for pulsed and resonant operation are shown in figure 6. For pulsed driving we used a MOSFET driver with current limiting 50 Ohm resistors. The pulse amplitude, width, and frequency were varied using a pulse generator. For the resonant operation, sinusoidal excitation was used with frequency ranging from 100 kHz to 15 MHz. The driver is much simpler compared to conventional ultrasonic motors that require two or more phases. The voltage ranged from 50 to 250 V and 4 to 20 V<sub>PP</sub> for pulsed and resonant drive respectively over the PZT.

To verify the theory of operation and to visualize the hub plate modes, a interferometer set-up shown in figure 7 was used. The light beam reflected from the surface of the hub and the rotor edge is interfered with a reference beam, originating from the beam splitter in the optical column. Interferometric measurements of micromachined beams have been performed before by measuring the interference of the reflected signals from different surfaces [11]. The interferometer together with the high speed camera allowed us to visualize the rotating standing waves on the hub.

## V. EXPERIMENTAL RESULTS

### A. Actuation in STP

By applying voltage pulses with magnitude of 120 volts continuous motor operation was demonstrated. The actuation was found to be effected by the pulse width. Pulses shorter than 200 ns did not result in continuous rotation. Also, there was no benefit in operating with longer than 800 ns pulses. This is in agreements with the simulations that suggested 600 ns pulses to be optimal for actuation. The pulsing rate was varied between 100 and 450 Hz with pulse width of 450ns. The resulting rotation speed of the rotor driven in atmospheric pressure is shown in figure 9 with maximum rotation speed of 3 RPM. The rotation rate increases initially linearly and then saturates and decreases. This suggests that at high pulse rate the effect of the individual pulses intermix reducing momentum transfer.

The resonant drive was demonstrated by driving the rotor at various resonant frequencies. The control over the rotation direction was obtained by slightly adjusting the drive frequency: driving the rotor slightly below the resonance results in different rotation direction than driving above resonance. As shown in figure 8, there are many resonances below 1 MHz. These resonances correspond to flexural and longitudinal vibrations of the PZT-silicon composite. Most of these resonances could be used to drive the rotor with typical driving voltage of 15 V<sub>PP</sub>. The excitation of many hub resonances is possible because the rotor was placed at the center of the die, which is a node for many die resonance modes. However, even more promising were the thickness mode resonances above 1 MHz. Continuous operation was demonstrated at these frequencies as shown in figures 10 and 11 with drive voltage as low as 4 V<sub>PP</sub>. The maximum rotation speed was 105 RPM with drive voltage of 7 V<sub>PP</sub> for rotor driven at 7.6 MHz. the quadratic increase in speed vs. voltage indicates that the role of acoustic streaming in STP. Increasing voltage above this did not increase rotation rate. There are two possible explanations for this behavior. It is possible that at higher power levels the energy is lost due to increase in losses in PZT. Alternatively explanation is that the actuation is due to acoustic streaming as discussed in section II. The area-compensated power consumed by the motor at resonance was 200 microwatts. The reliability of the device was tested by operating it continuously for four days in uncontrolled room environment. The device kept rotating without failing.

### B. Actuation in Vacuum

To investigate the effect of acoustic streaming and viscous drag forces the experiments were repeated in vacuum ( 200 mTorr). In vacuum the rotor spun about 10 to 100 times faster and in the same direction but made erratic back-steps as the pulse width was changed. The back steps indicate that the actuation is not purely frictional but

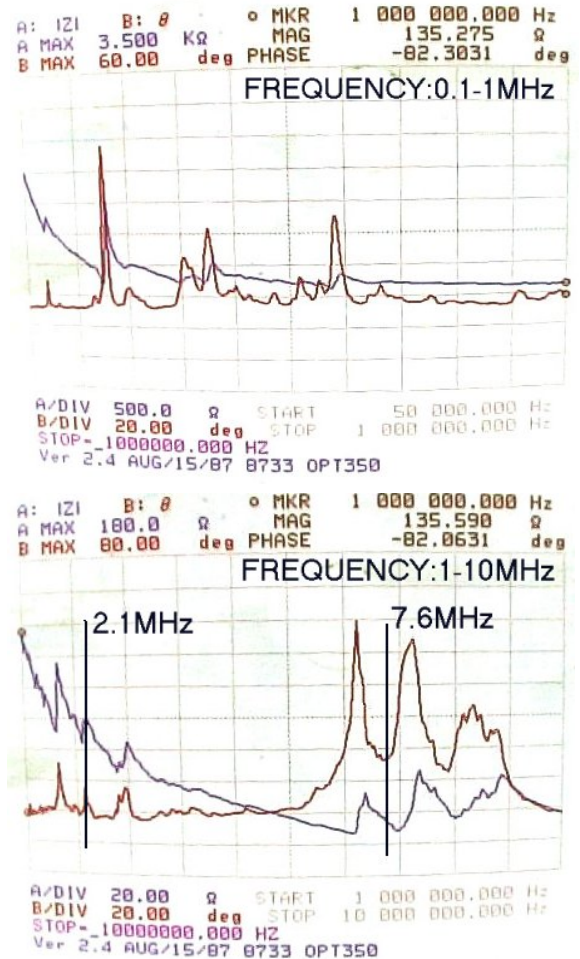


Figure 8: Frequency response of the PZT/silicon composite measured with HP4194 impedance analyzer

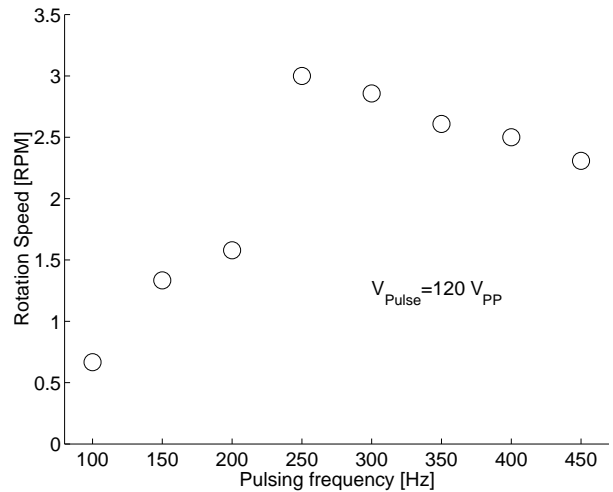


Figure 9: Rotation speed for a pulsed rotor

impact transfer is also important. Unfortunately there was no mark on the rotor to reliably measure the rotation speed at this high RPM. We are currently redesigning the rotor to carry out this measurement.

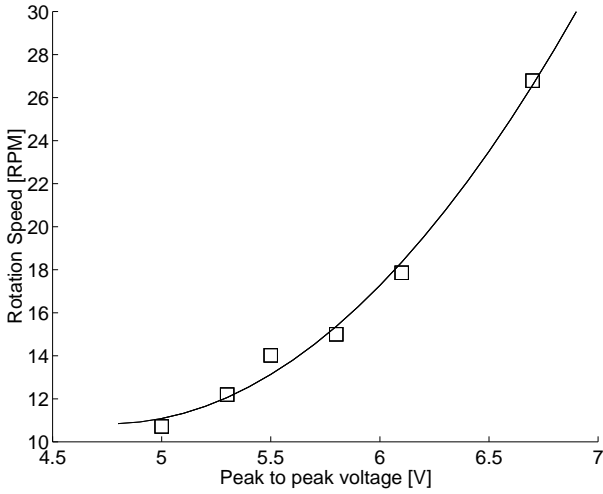


Figure 10: RPM for a rotor driven at 6.6 MHz.

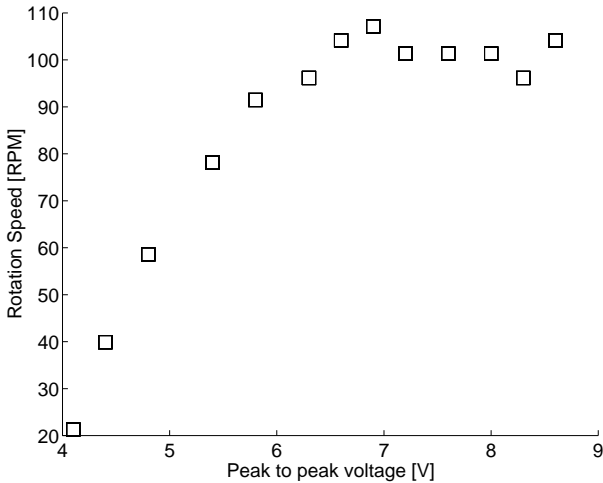


Figure 11: RPM for a rotor driven at 7.6 MHz.

In vacuum acoustic streaming cannot be responsible for actuation and the actuation must be due to direct contact. After operating the rotor continuously for several hours in vacuum, significant wear was observed on the top of the rotor around the edge of the hub holding it in place, indicating the role of the rub-rotor interaction. Eventually the rotor stopped operating after getting permanently stuck on the hub. The lack of wear at atmospheric pressure indicates that an air cushion exists between the rotor and the hub. The air cushion also smoothens the rotor operation, a fact verified experimentally.

The hub resonant modes were observed in the interferometric setup. Two images are shown in figures 12. The individual mode shape are captured during transient reduction of drive power to the resonator. The resonant mode captured at the 2.1 MHz resonance contains 8 nodes while the plate resonance at 7.6 MHz resonance has 16 nodes. The two-fold increase in the number of nodes by an approximate four-fold increase in frequency is expected from the plate quadratic dispersion relationship be-

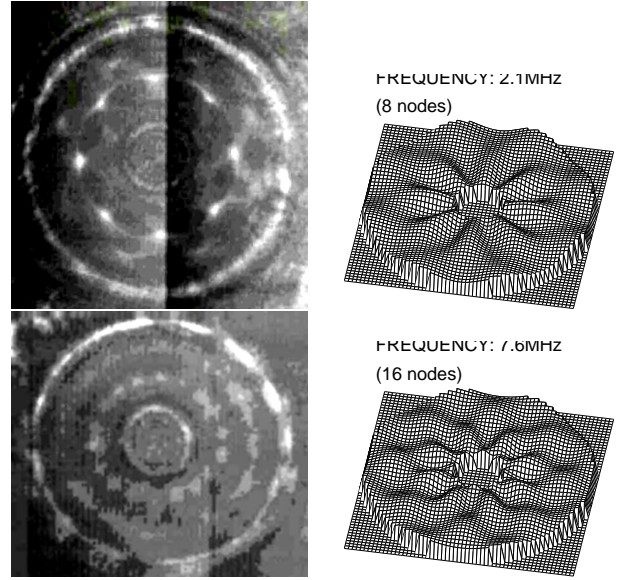


Figure 12: Interferometric image of resonant actuated rotor in vacuum showing nodes and corresponding simulated mode of the hub.

tween the wavenumber and frequency for thin plates [12]. During motor operation, the node locations were averaged out by the camera producing rings as shown in figure 13. Studies on macro size ultrasonic motors actuated by acoustic streaming show that the rotation speed increases with higher order vibration modes [13] due to higher momentum transfer rate. This is in agreement with the fact that the highest studied drive frequency in our experiments resulted in the highest rotation speed.

## VI. DISCUSSION AND CONCLUSIONS

We have shown first ever completely surface micromachined ultrasonic rotor. It operates with a single-phase drive, which is different than the many electrodes needed for traditional ultrasonic motors. Furthermore, extended operation in air with 4 Vpp operation consuming only 200 microwatts of power implies that integrated digital circuits could be used to drive the motor. Adjusting the operating frequency could change the motor rotation direction. This is believed to be due to the effective change of the

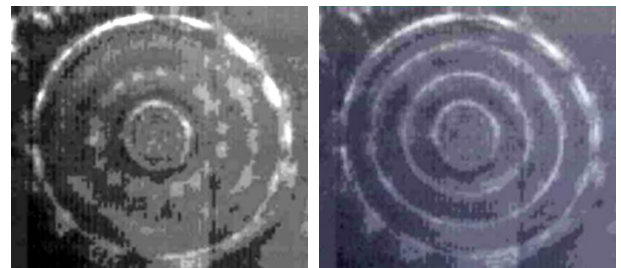


Figure 13: The nodal pattern (left) becomes rings (right) as the standing waves start rotating at a high speed.

momentum transfer relationship. The motor could also be used a stepper motor under pulsed actuation with voltages ranging from 50 to 100 V<sub>pp</sub> for a duration on 300 to 600 ns. The ability to drive a highly geared down rotor at higher rotation rates implies the capability to drive large loads. More experiments are underway to quantify the torque/rotation rate relationship.

Remarkably, stiction was not a problem in air for continuous operation over four days. We believe that this robustness is a result of constant ultrasonic vibration and an air cushion, which prevents repeated impacts between parts. This result signifies the possibility of a motor with high reliability and long-lifetime. This robustness was not seen for vacuum operation where frequent impacts between the hub and rotor resulted in surface erosion.

The motor does not consume any chip real estate compared to the more traditional electrostatic and thermal surface actuators. This motor will allow for more effective use of the chip area. The actuation is done via a commercially available piezoelectric plate attached on unused backside of the silicon die. Unlike the electrostatic and thermal actuation schemes, the actuation proposed here does not require interconnects. This feature enables the remote actuation of surface micromachines sealed inside environments not compatible with interconnects. The low temperature adhesive attachment of the piezoelectric die is compatible with any surface micromachining process. Hence, micromachines made anywhere can be actuated using ultrasonic pulses. We have actuated structures made using both the MUMPS and the SUMMiT IV process.

The electronic drive circuitry is similar to one used to drive capacitive loads and amenable to standard CMOS driver design. In the near future we aim to develop a better model of the mechanisms of the rotor operation using interferometric images and additional controls on the mechanical boundary conditions. By designing new motor designs with different gap spacing and rotor sizes we will be able to deduce the importance of impact actuation and acoustic streaming induced actuation.

## VII. ACKNOWLEDGMENTS

We acknowledge the Wisconsin Center for Applied Microelectronics (WCAM) for technical support and the Wisconsin Alumni Research Foundation (WARF) for funding. Devices were fabricated by the Sandia National Lab. Sandia is a multiprogram laboratory operated by Sandia Corporation, a Lockheed Martin Company, for the United States Department of Energy under Contract DE-AC04-94AL85000.

## REFERENCES

- [1] S. Ueha and Y. Tomikawa, *Ultrasonic Motors: Theory and Applications*, Clarendon Press, 1993.
- [2] R. Moroney, R. White, and R. H. R., "Ultrasonic Micromotors", *IEEE 1989 Ultrasonics Symposium Proceedings*, pp. 745–748, Montreal, Que., Canada, Oct. 1990.
- [3] R. Moroney, R. White, and R. H. R., "Ultrasonic Micromotors: Physics and Application", *Proceedings. IEEE Micro Electro Mechanical Systems*, pp. 182–187, Napa Valley, USA, Feb. 1990.
- [4] A. Flynn, L. Tavrow, S. Bart, R. Brooks, D. Ehrlich, K. Udayakumar, and L. Cross, "Piezoelectric Micromotors for Microrobots", *IEEE 1990 Ultrasonics Symposium Proceedings*, pp. 1163–1172, Honolulu, USA, 1990.
- [5] A. Flynn, L. Tavrow, S. Bart, R. Brooks, D. Ehrlich, K. Udayakumar, and L. Cross, "Piezoelectric Micromotors for Microrobots", *Journal of Micromechanical Systems*, vol. 1(1), pp. 44–51, Mar. 1992.
- [6] A. Lal and R. M. White, "Silicon Microfabricated Horns for Power Ultrasonics", *Sensors and Actuators*, vol. A54(1-3), pp. 542–546, Jun. 1996.
- [7] A. E. M. Koch and A. Brunschweiler, "The Dynamic Micropump Driven with a Screen Printed PZT Actuator", *Journal of Micromechanics and Microengineering*, vol. 8(2), pp. 119–122, Jun. 1998.
- [8] V. Kaajakari and A. Lal, "Pulsed Ultrasonic Release and Assembly of Micromachines", *The 10th International Conference on Solid-State Sensors and Actuators*, pp. 212–215, Sendai, Japan, Jun. 7-10, 1999.
- [9] V. Kaajakari and A. Lal, "Pulsed Ultrasonic Actuation of Polysilicon Surface Micromachines", *IEEE International Ultrasonics Symposium*, Ceasars Tahoe, Nevada, USA, Oct. 1999.
- [10] M. S. Rodgers, J. J. Sniegowski, S. L. Miller, C. C. Barron, and P. J. McWhorter, "Advanced Micromechanisms in a Multi-Level Polysilicon Technology", *Proc. of SPIE Micromachined Devices and Components III*, pp. 120–130, Austin, TX, USA, Sep. 1997.
- [11] M. P. de Boer and T. A. Michalske, "Accurate Method for Determining Adhesion of Cantilever Beams", *Journal of Applied Physics*, vol. 86(2), pp. 817–827, Jul. 1999.
- [12] K. Graf, *Wave Motion in Elastic Solids*, Dover, 1991.
- [13] J. Hu, K. Nakamura, and S. Ueha, "An Analysis of a Noncontact Ultrasonic Motor with an Ultrasonically Levitated Rotor", *Ultrasonics*, vol. 35(6), pp. 459–467, Sep. 1997.